ACI MATERIALS JOURNAL TECHNICAL PAPER

Title No. 114-M21

Concrete Damage under Fatigue Loading in Uniaxial Compression

by Benard Isojeh, Maria El-Zeghayar, and Frank J. Vecchio

Despite rigorous efforts in the derivation of various fatigue damage models for concrete, damage predictions of sufficient accuracy are still limited to loading conditions similar to those of the experiments used for developing the models. Most models are void of salient factors affecting the fatigue behavior of concrete such as frequency, stress ratio, and loading waveform, and the approaches used in developing such models tend to be rudimentary. Therefore, further investigation is required.

In this study, damage models are expressed for residual concrete strength and fatigue secant modulus using experimental data from tested cylindrical specimens, a damage function, and a stress-life model in the literature. The number of cycles leading to failure, required for normalizing the fatigue cycles for each specimen, is obtained using a proposed secondary strain rate model. The aforementioned influencing factors incorporated into the damage function result in robust models that account for variations in loading parameters.

Keywords: compressive strength; damage; fatigue; fatigue secant modulus; residual concrete strength; strain evolution; variable loading.

INTRODUCTION

During fatigue loading, the properties of concrete undergo alterations that result in damage. The progressive damage of a concrete element can be observed from the evolution of various deformation parameters, such as total strain, residual strain, stiffness degradation, strength degradation, heat dissipation due to microcrack, crack growth, and speed of sound in concrete.[1,2] Based on previous investigations on the fatigue behavior of concrete, the damage evolution for each parameter is nonlinear.[3-7]

The fatigue behavior of concrete is influenced by various factors, unlike the fatigue behavior of steel reinforcing bars. Investigations conducted by Aas-Jakobsen,[8] Murdock and Kesler,[9] Hilsdoft and Kesler,[10] Awad and Hilsdorf,[11] and Oh[12] have shown that the increase in maximum fatigue stress results in a decrease in the number of cycles to failure, while a higher minimum stress level corresponds to an increase in the number of cycles to failure. According to Ople and Hulsbos[13] on stress gradient (eccentricity in fatigue loading), the number of cycles to failure increases as the eccentricity of loading increases.

As reported in previous investigations, an overestimation of the fatigue life will occur if a fatigue model developed using a higher frequency of loading compared to that of the real structure is used in an analysis or design. Investigations conducted on the influence of frequency by Graf and Brenner,[14] Spark and Menzies,[15] Raithby and Galloway,[16] Holmen,[17] Naik et al.,[18] and Zhang et al.[19] all indicate that the number of cycles leading to failure decrease as the frequency of loading decreases. This behavior has been observed to be more pronounced as the maximum fatigue stress level increases. For higher fatigue stress levels, the behavior of concrete depends on the fatigue cycles and on the duration of loading where creep effects become significant, leading to a reduction in the fatigue life.[10] On the contrary, Takhar et al.,[20] based on statistical analysis, concluded that there was no significant difference between tests conducted at a loading frequency of 20 cycles per minute and 60 cycles per minute for stress levels of 0.8 and 0.9 (fractions of average compressive strength).

It has also been reported in the literature that the shape of the waveform used in fatigue loading influences the fatigue life. However, the influence is more prominent at maximum stress levels equal to or greater than 0.8, or at maximum stress levels that result in failure at cycles less than or equal to 1000. From observations, the number of failure cycles with a sinusoidal waveform will be about half of the number of failure cycles for a triangular waveform, while the number of failure cycles for a rectangular waveform will be about one-sixth of the number of cycles to failure for a sinusoidal waveform under the same stress level.[2,21]

The impact of stress reversal under fatigue loading was investigated by Zhang et al.[19] on 171 beams with seven stress ratios, including negative stress ratios. The ratios were combined with 13 stress levels. The stress-life curves (S-N), obtained by plotting the stress level against the failure cycle for each specimen, portrayed reduction in the fatigue life of the concrete specimens as the stress ratio reduced.

The effects of other factors such as the shape of the specimen, the water-cement ratio (w/c), aggregate type and gradation, concrete strength, curing conditions, age at loading, and moisture conditions that affect concrete can be removed by normalizing the stress levels with the ultimate capacity of concrete under static load.[16,22-25] This concept reduces the number of factors considered in analytical models for predicting the behavior of concrete elements under fatigue load to the loading parameters alone.[2]

The perception of damage evolution of a material provides a conceptual basis by which the degradation of the mechanical properties of concrete and the corresponding physical defor-

ACI Materials Journal, V. 114, No. 2, March-April 2017.

MS No. M-2015-361.R3, doi: 10.14359/51689477, received July 19, 2016, and reviewed under Institute publication policies.

mation can be correlated. Obtaining the damage evolution for parameters such as residual strength and secant stiffness may require discrete test points from a number of tested specimens.[26-29] To obtain the discrete test points, specimens are loaded cyclically to different numbers of cycles before failure; thereafter, the observed deformation parameter at given cycles are plotted against the normalized number of cycles.

Due to the stochastic nature of concrete,[30-32] the actual number of cycles to failure for each specimen is different even under the same magnitude of fatigue load. Hence, the use of S-N models in estimating the number of cycles to failure for normalizing the specified tests cycles[33-35] is inappropriate, and the corresponding models developed do not portray the actual parametric damage evolution.

According to Sparks and Menzies,[15] Cornelissen and Reinhardt,[28] and Taliercio and Gobbi,[5] a correlation exists between the secondary strain rate and the number of cycles leading to failure. As such, provided the secondary strain rate can be obtained for each specimen tested, the failure cycles can be estimated.

At the final damage states of concrete specimens, the fatigue secant modulus at failure has been reported to converge at approximately 60% of the initial fatigue secant moduli.[2,17] In a similar manner to the fatigue secant modulus, the strength of composite materials also deteriorates under fatigue loading. Hence, it has been reported that the same damage evolution model can be used for residual strength and stiffness.[34] However, the initial stage of fatigue loading of concrete is characterized by a slight increase in strength.[5,27,33,37] This phenomenon is attributed to the consolidation or the closing up of microvoids in concrete at the initial stage of fatigue loading.[29] The increase in strength may also be attributed to the stochastic nature of concrete.[30-32]

Once strength damage initiates, an increase in damage will be observed in subsequent cyclic loading; thereafter, loading a concrete specimen monotonically to failure will result in a lower compressive strength.

In this paper, the stress ratios for the experiments conducted are either equal to or greater than zero; hence, no fatigue stress reversal is considered. In addition, a sinusoidal waveform is used for all fatigue tests conducted.

To obtain normalized fatigue cycles, the numbers of cycles to failure of tested specimens were estimated using the secondary strain rate concept. From a damage function expressed by Gao and Hsu,[37] modified robust damage models that incorporate influencing fatigue factors from an S-N model[19,38] are developed for concrete strength and residual fatigue secant modulus using data from tested specimens.

RESEARCH SIGNIFICANCE

This investigation incorporates the concept of secondary strain rate for obtaining fatigue life in the formulation of improved damage models for concrete in compression. Further, key fatigue factors from an existing S-N model (frequency, stress ratio, loading waveform) are incorporated; hence, the combined models are suitable for a wide variety of fatigue loading conditions for concrete structures. The models proposed can be implemented into general concrete constitutive models for predicting strength and stiffness deterioration and improved fatigue analysis of concrete structures.

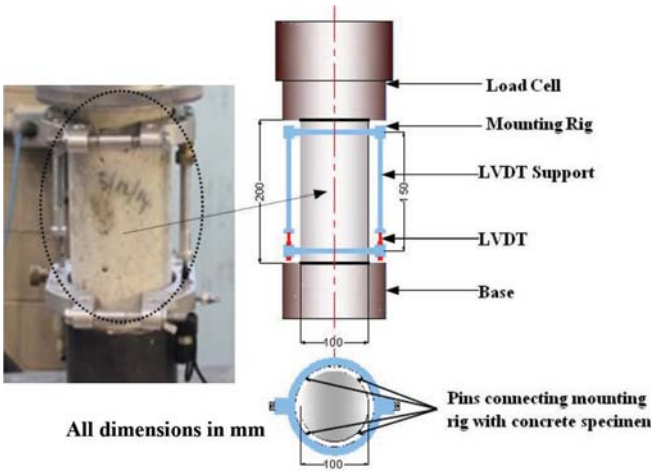

Fig. 1—Fatigue loading setup.

Table 1—Average compressive strength and corresponding strain

Batch (No. of specimens)	Average compressive strength, MPa	Average corresponding strain (× 0.001)	Mixture ratio	*w/c*
1 (5)	52.8	2.01	1:2:2*	0.5
2 (3)	55.8	2.00	1:2:2*	0.5
3 (3)	46.2	1.95	1:2:3*	0.5
4 (5)	23.1	1.52	1:2:4*	0.6

*Cement:sand:coarse aggregate.

EXPERIMENTAL INVESTIGATION

Experiments were conducted on concrete cylinders to develop a secondary strain rate model and to observe subsequent residual strengths and fatigue secant moduli as the number of fatigue loading cycles increased. The secondary strain rate is defined as the rate of change in maximum fatigue strain per unit cycle within the linear portion of the strain evolution profile (secondary stage). For the residual strength and fatigue modulus, each specimen was tested to a different number of cycles less than the actual cycles leading to failure.

The tests were conducted using servo-hydraulic testing equipment having a loading capacity of 1000 kN (224.8 × 10^3 lbf). The loading equipment was programmed to generate a pulsating load of a continuous sinusoidal waveform throughout the test duration. Each specimen was mounted with attached linear variable displacement transducers (LVDTs), as shown in Fig. 1. The LVDTs were used to measure average strains in the specimens throughout the duration of the fatigue tests.

Concrete cylinders (38 specimens) with dimensions of 100 mm diameter x 200 mm height (4 x 8 in.) were subjected to uniaxial fatigue loading in compression. Prior to the fatigue tests, concrete specimens (at least three per batch) were tested statically to obtain the average compressive strength, as shown in Table 1. The stress levels (maximum and minimum stresses) for the fatigue tests were taken as percentages of the average compressive strength.

Table 2—Specimen fatigue parameters and test failure data

Specimen	Compressive strength f_c', MPa (psi)	Stress level, % of f_c'	Frequency, Hz	Number of cycles to failure (N_f)	logN_f
E5	52.8 (7660)	74	5	12,210	4.09
E8	52.8 (7660)	74	5	10,180	4.01
E13	52.8 (7660)	74	5	8720	3.94
E21	52.8 (7660)	74	5	8460	3.93
E3	52.8 (7660)	74	5	5640	3.75
G4	46.2 (6700)	74	5	4690	3.67
G11	46.2 (6700)	74	5	4600	3.66
E10	52.8 (7660)	69	5	25,180	4.4
E15	52.8 (7660)	69	5	20,500	4.31
H16	55.8 (8090)	80	5	747	2.87
H17	55.8 (8090)	80	5	3530	3.55
I1	23.1 (3350)	75	5	3220	3.51
I5	23.1 (3350)	75	1	4910	3.69
I6	23.1 (3350)	75	5	1560	3.19
I8	23.1 (3350)	75	1	3030	3.48
I10	23.1 (3350)	75	1	5011	3.70

Table 3—Strength and secant modulus degradation test data

Specimen	Initial compressive strength f_c', MPa (psi)	Number of cycles before static loading	Residual strength after static loading, MPa (psi)	Residual fatigue modulus, MPa (psi × 10^3)
E22	52.8 (7660)	430	54.9 (7960)	68869 (9990)
E9	52.8 (7660)	430	54.4 (7890)	58088 (8420)
E20	52.8 (7660)	860	55.1 (7990)	65124 (9440)
E11	52.8 (7660)	860	53.0 (7690)	58806 (8530)
E4	52.8 (7660)	5150	55.3 (8020)	62047 (9000)
E17	52.8 (7660)	7730	52.3 (7580)	55211 (8010)
E1	52.8 (7660)	8160	53.4 (7740)	53333 (7740)
E2	52.8 (7660)	3480	46.5 (6740)	44222 (6410)
G3	46.2 (6700)	5550	41.7 (6050)	33433 (4850)
G7	46.2 (6700)	5880	38.6 (5600)	30136 (4370)
G8	46.2 (6700)	18080	36.3 (5260)	31402 (4550)
G9	46.2 (6700)	6180	32.9 (4770)	25759 (3740)
H1	55.8 (8100)	5000	51.4 (7450)	50244 (7290)
H3	55.8 (8100)	1200	58.1 (8430)	61804 (8960)
H9	55.8 (8100)	3000	56.2 (8150)	57622 (8360)
H4	55.8 (8100)	6120	45.6 (6610)	45055 (6530)
H5	55.8 (8100)	5840	49.2 (7140)	43871 (6360)
H6	55.8 (8100)	7900	44.7 (6480)	42842 (6210)
H7	55.8 (8100)	4680	36.1 (5240)	37169 (5390)
H11	55.8 (8100)	6710	52.5 (7610)	54342 (7880)
H14	55.8 (8100)	9870	46.8 (6790)	38750 (5620)
H15	55.8 (8100)	8660	37.9 (5500)	33306 (4830)

*Failed before reaching maximum fatigue load applied.

The maximum stress level, the concrete strength, and the loading frequency were variables in this experimental investigation. Maximum stress levels of 0.69 to 0.80, as fractions of the average compressive strength, were used as the fatigue loads. Sixteen specimens were loaded to failure to observe the evolution of the maximum strain as indicated in Table 2, while 22 specimens, as indicated in Table 3, were loaded to

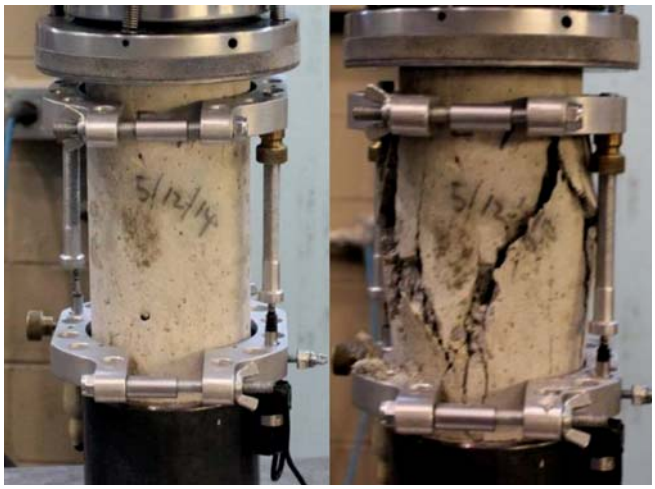

Fig. 2—Concrete specimen in undamaged and damaged states.

different numbers of cycles that were less than the number of cycles to failure at a constant maximum stress level of 0.74.

The 22 specimens tested were used to observe the evolution of strength and fatigue secant modulus of concrete. Although the value of 0.74 was chosen arbitrarily, it falls within the range for high cycle fatigue. The 22 specimens tested under fatigue loading were subsequently loaded monotonically to failure. For the specified load levels, a frequency of 5 Hz (1.1 lbf) was used for all batches. A frequency of 1 Hz (0.22 lbf) was used for testing three specimens from the fourth batch. For all fatigue tests conducted, a constant minimum load of 5 kN (1.1 lbf) was used.

Test specimens

The concrete specimens were made from portland cement (general use [GU]), sand, and limestone aggregates (10 mm [0.4 in.] maximum size) with three different mixture proportions. The concrete from the first two batches, as indicated in Table 1, were cast using a mixture proportion of 1:2:2 (cement:sand:coarse aggregate) with a water-cement ratio (*w*/*c*) of 0.5. For the third and fourth batches, mixture proportions of 1:2:3 with a *w*/*c* of 0.5 and 1:2:4 with a *w*/*c* of 0.6 were used, respectively. The fineness modulus of the sand used was estimated to be 2.6. The slumps observed from the fresh concrete from all batches were 100 to 150 mm (4 to 6 in.). The static strengths of concrete after curing for 28 days were obtained from each batch, while the fatigue tests were conducted 30 to 40 days after cast.

The first, second, third, and fourth batches were denoted as E, H, G, and I, respectively, as indicated in Table 2. The number added to each alphabet in the table indicates the number assigned to the specimen before testing.

Results

At the initial stage of fatigue loading, increase in strain at a decreasing rate was observed due to the closing up of concrete pores and microcracks between aggregates and cement mortar. Subsequently, the rate of strain evolution was constant while microcracks within the cement mortar increased. Within the last stage of fatigue damage evolution, the microcracks merged to form macrocracks. Similar to

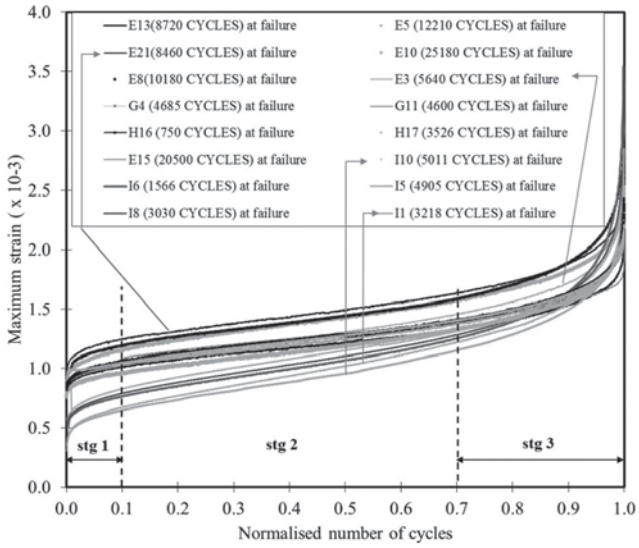

Fig. 3—Maximum strain evolution.

static loading, these cracks (hairlines) were obvious on the surfaces of the concrete specimens and were approximately parallel to the direction of loading. Further, the ends of these macrocracks merged and developed a failure plane that resembled a fault (Fig. 2). The numbers of cycles leading to failure were recorded for the 16 specimens tested and are given in Table 2. The standard deviations (in terms of the logarithm of the number of cycles to failure, N_f) observed for the four different stress levels (74%, 75%, 69%, and 80%) are 0.17, 0.21, 0.06, and 0.48, respectively. The respective mean values are 3.86, 3.51, 4.36, and 3.21. However, the standard deviation of the error ($\log N_f$) between the experimental data and the model by Zhang et al.[19] is 0.26 and the model prediction (in logarithm) is 3.80 for 74% stress level.

Maximum strain evolution

The strain evolutions for the 16 specimens tested to failure under fatigue loading were plotted against the normalized number of cycles, as shown in Fig. 3. The shapes or profiles of the strain evolutions were similar, irrespective of the concrete strength and stress level. The three stages of the strain evolution shown in Fig. 3 for the stress levels used are also in agreement with previously reported observations.[2-7] The first stage, within 10% of the total number of cycles to failure, indicates a nonlinear deformation of concrete at a decreasing rate. The second stage is characterized with a constant rate of deformation within a range of approimately 70% of the fatigue life, while the last stage is characterized with an increasing rate of damage leading to failure. This was observed to be within the last 30% of fatigue life.

MODEL FORMULATION

A major challenge in the development of residual strength and fatigue modulus models involves the estimation of the expected fatigue life for each specimen, because the applied fatigue load is usually stopped after a given number of cycles before failure occurs. In the literature, S-N models are generally used to normalize the tests cycles. As such, the plot of the residual strength against failure cycles obtained is often not appropriate. This is due to the fact that the actual

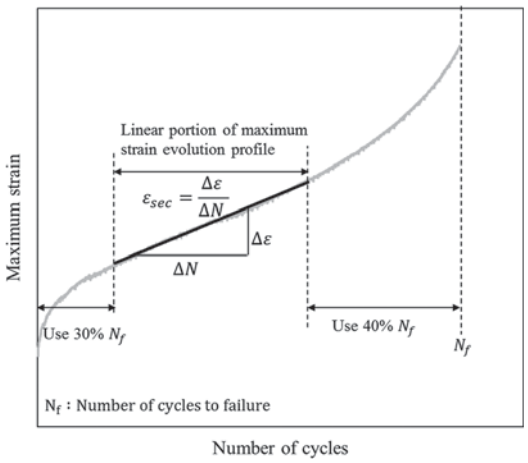

Fig. 4—Plot of maximum strain against number of cycles.

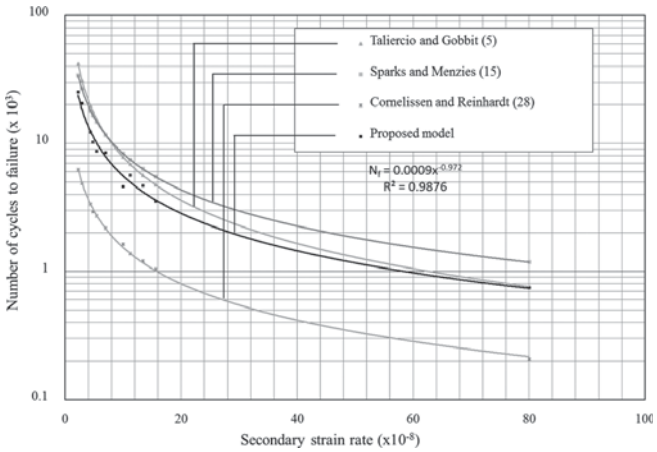

Fig. 5—Logarithm of number of cycles to failure against secondary strain rate.

number of cycles to failure of some of the specimens may be higher or lower than the value estimated using an S-N model. As such, an approach for estimating the number of cycles to failure for each specimen is required.

Relationship between secondary strain rate and number of cycles to failure

The secondary strain rates (ε_{sec}) for 11 specimens (high-strength concrete) out of the 16 specimens tested to failure were all estimated, as illustrated in Fig. 4. The logarithms of fatigue life (N_f) were plotted against the secondary strain rates (ε_{sec}), as indicated in Fig. 5. Using the experimental data, a model was proposed (Eq. (1)). Figure 5 also shows a comparison of the model with other models in the literature. The coefficients in the models were obtained based on best-fit curve. To show the predictability of the model, data from fatigue tests at different loading parameters from different researchers were obtained and included in the plot, as shown in Fig. 6.[5,15,39] In addition, a prediction interval (using 95% confidence interval) is also shown in Fig. 6 (log-log plot). However, due to the scarce data for very high cycles to failure in the literature, fatigue strain evolution tests involving very high fatigue life are also required for corroboration.

$$N_f = 0.0009(\varepsilon_{sec})^{-0.972} \quad (1)$$

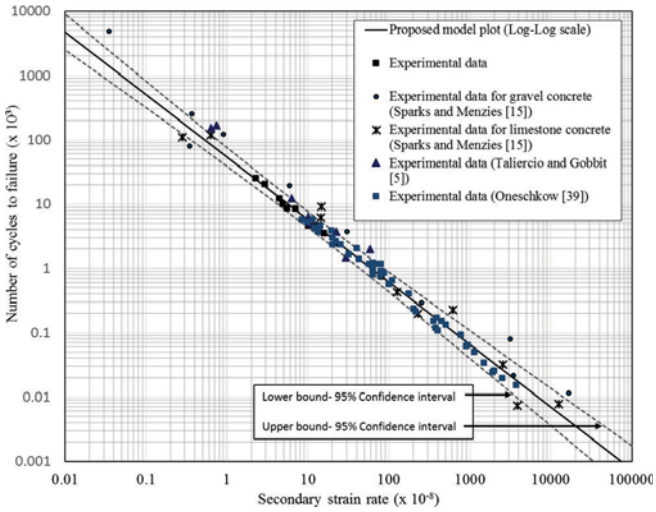

Fig. 6—Verification of strain rate model for high number of cycles.

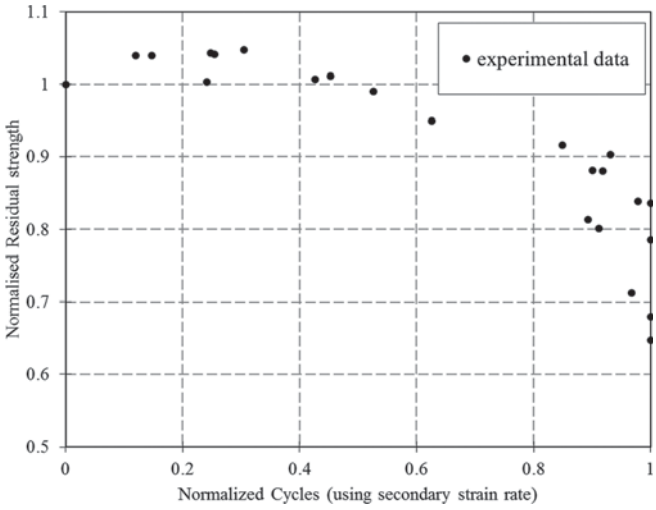

Fig. 7—Normalized residual strength against normalized cycles (second strain rate approach).

The proposed model was used to estimate the failure cycles for the 22 specimens to obtain a plot of the residual concrete strength against the corresponding normalized number of cycles for each specimen. The plot of the normalized residual strength against the normalized number of cycles in Fig. 7 and 8 were obtained using the proposed model (Eq. (1)) and the Aas-Jakobsen's model [8] (Eq. (2)), respectively. It can be observed from the figures that the actual degradation path is well represented using the proposed model.

$$\Delta f/f_c' = 1 - \beta(1 - R)\log N_f \quad (2)$$

In Eq. (2), β is a material parameter and R is the ratio of the minimum stress level to the maximum stress level. The ratio of Δf to f_c' is the stress level, which is the applied loading stress divided by the average compressive strength of the concrete considered. On the other hand, the residual strength of concrete corresponds to the actual stress at which a fatigue-damaged specimen will fail when loaded monotonically under static condition. After considerable damage of concrete due to fatigue loading, the residual strength

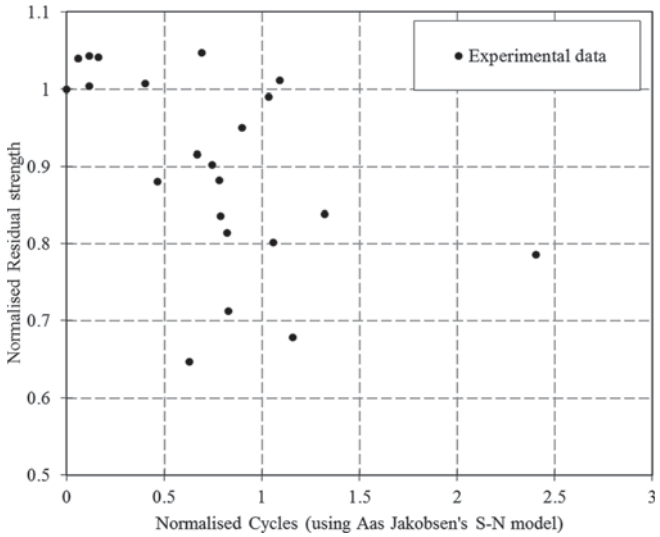

Fig. 8—Normalized residual strength against normalized cycles (S-N model).

of concrete is usually lower than the actual compressive strength in its undamaged state.

Strength and stiffness degradation under fatigue loading

During the initial stage of the fatigue loading, the residual strengths of the concrete specimens were observed to increase. This observation has also been reported in the literature on fatigue tests of concrete specimens in compression. However, based on the damage path depicted by the experimental data points, obvious strength degradation began within the secondary stage of the damage evolution (Fig. 7). Figure 9 and Eq. (3) and (4) describe the approach taken for estimating the static and fatigue secant moduli of concrete (E and E_{sec}, respectively) for each of the 22 specimens tested.

The fatigue secant modulus degradation began within the primary stage of damage and at a faster rate compared to the residual strength degradation. The degradation of the normalized fatigue secant moduli is also shown in Fig. 10. Toward failure, an abrupt drop was observed in the residual fatigue moduli data points.

$$E = \frac{\sigma_{max} - \sigma_{min}}{\Delta\varepsilon} \tag{3}$$

$$E_{sec} = \frac{\sigma_{max} - \sigma_{min}}{\varepsilon_{cv}} \tag{4}$$

Damage evolution model for concrete strength and fatigue secant modulus

From the fundamentals of damage mechanics, the rate of fatigue damage per cycle is a function of the number of cycles, stress level, and a damage variable. From Gao and Hsu,[37] the rate of change of damage per fatigue cycle is expressed as

$$\frac{\delta D}{\delta N} = F(N, \Delta f, D) = k_1 \exp\left(\frac{s\Delta f}{f_c'}\right) N^K \tag{5}$$

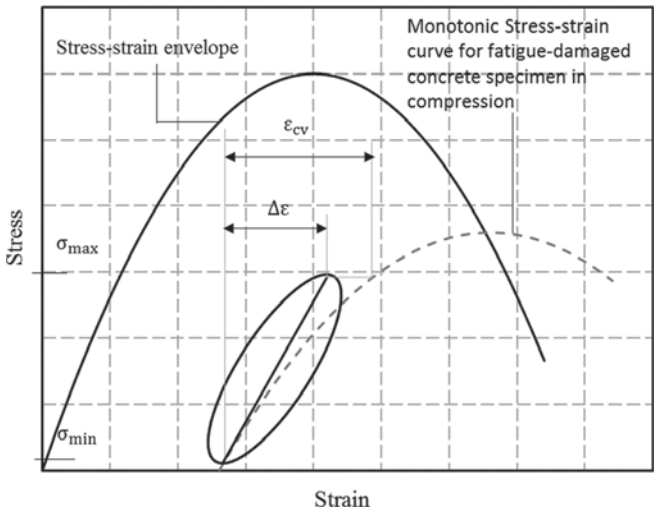

Fig. 9—Static and fatigue secant moduli.

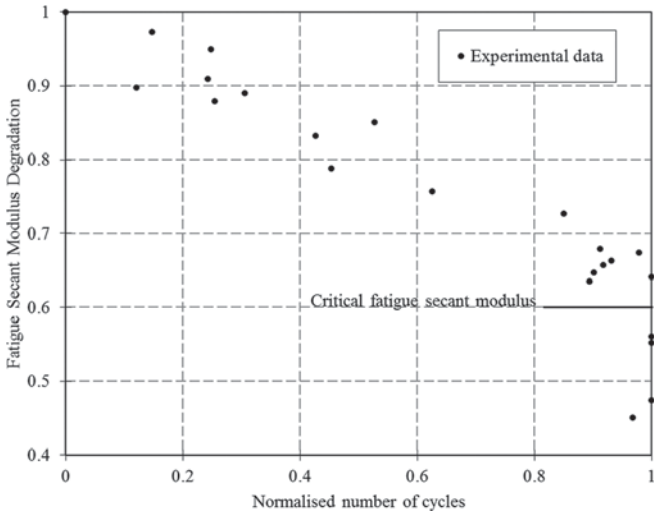

Fig. 10—Degradation of residual fatigue secant modulus.

By integrating Eq. (5) with respect to N,

$$D = k_1 \exp\left(\frac{s\Delta f}{f_c'}\right) \frac{N^{K+1}}{(K+1)} \tag{6}$$

At failure, damage $D = D_{cr}$.

$$D_{cr} = k_1 \exp\left(\frac{s\Delta f}{f_c'}\right) \frac{(N_f)^{K+1}}{(K+1)} \tag{7}$$

Rearranging Eq. (7),

$$\frac{\Delta f}{f_c'} = \frac{1}{s} \ln \frac{D_{cr}(K+1)}{k_1} - \frac{K+1}{s} \ln N_f \tag{8}$$

To account for the influence of loading parameters such as frequency, waveform, and stress ratio, a modified Aas-Jacobsen' S-N model[8,38] (Eq. (9)), which considers various factors affecting the fatigue behavior of concrete, was implemented.

$$\frac{\Delta f}{f_c'} = C_f[1-\beta_2(1-R)\log N_f - \gamma_2 \log(\zeta N_f T)] \quad (9)$$

where

$$\beta_2 = 0.0661 - 0.0226R \quad (10)$$

and $\gamma_2 = 2.47 \times 10^{-2}$. ζ is a dimensionless coefficient that is taken as 0.15 for sinusoidal cycle,[2,38] C_f accounts for the loading frequency, and γ_2 is a constant that accounts for high stress level.

The modified S-N model for predicting failure cycles is expressed in a form similar to Eq. (8); hence

$$\frac{\Delta f}{f_c'} = C_f[1-\gamma_2 \log(\zeta N_f T)] - 0.434 C_f(\beta_2(1-R)) \ln N_f \quad (11)$$

where $\log N_f = 0.434 \ln N_f$.

Comparing Eq. (8) and (11),

$$\frac{(K+1)}{s} = 0.434 C_f(\beta_2(1-R)) \quad (12)$$

$$K + 1 = 0.434 s C_f(\beta_2(1-R)) \quad (13)$$

$$C_f(1-\gamma_2 \log(\zeta N_f T)) = \frac{1}{s} \ln \frac{D_{cr}(K+1)}{k_1} \quad (14)$$

$$D_{cr} \exp(-sC_f(1-\gamma_2 \log(\zeta N_f T)) = \frac{k_1}{K+1} \quad (15)$$

By substituting Eq. (13) and (15) into Eq. (6) and expressing the modified damage model in a form similar to the initially proposed model by Gao and Hsu,[37] then

$$D = D_{cr} \exp\left[s\left(\frac{\Delta f}{f_c'} - u\right)\right] N^v \quad (16)$$

$$u = C_f(1-\gamma_2 \log(\zeta N_f T)) \quad (17)$$

$$v = 0.434 s C_f(\beta_2(1-R)) \quad (18)$$

From Zhang et al.[19] on influence of loading frequency,

$$C_f = ab^{-\log f} + c \quad (19)$$

where a, b, and c are 0.249, 0.920, and 0.796, respectively, and f is the frequency of fatigue loading.

The residual strength of concrete and modulus damage at a given stress level can be obtained using the damage model. As observed, the damage model does not require the values of the constants K and k_1.

Using the damage model (Eq. (16)), parameters in constitutive equations can be modified to account for fatigue damage. From calibration using the tests data, the values of the parameter s (stress ratios between 0 and 0.5) for concrete strength and modulus damage can be obtained from Fig. 11. From the experiments conducted, the degraded fatigue modulus tends toward 60% of the initial modulus[2,17] (Fig. 10). As such, the critical damage value D_{cr} for the concrete fatigue secant modulus is taken as 0.4. As observed from the experimental data in Fig. 12, the residual strength of concrete at failure tends toward 0.65; hence, the damage value for the residual strength of concrete is taken as 0.35.

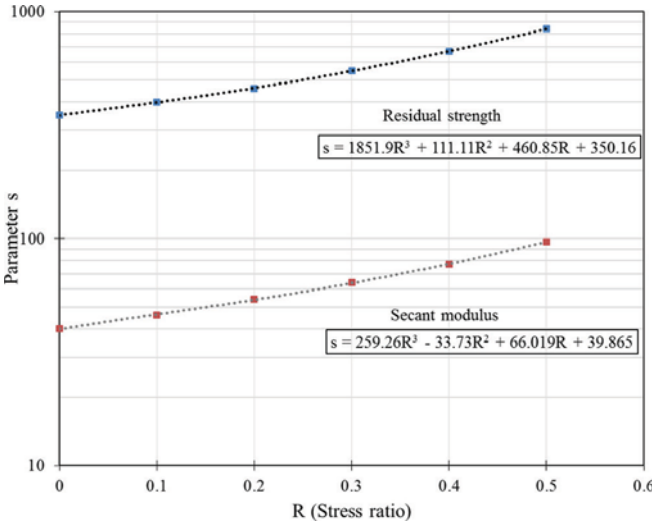

Fig. 11—Estimation of damage parameter s.

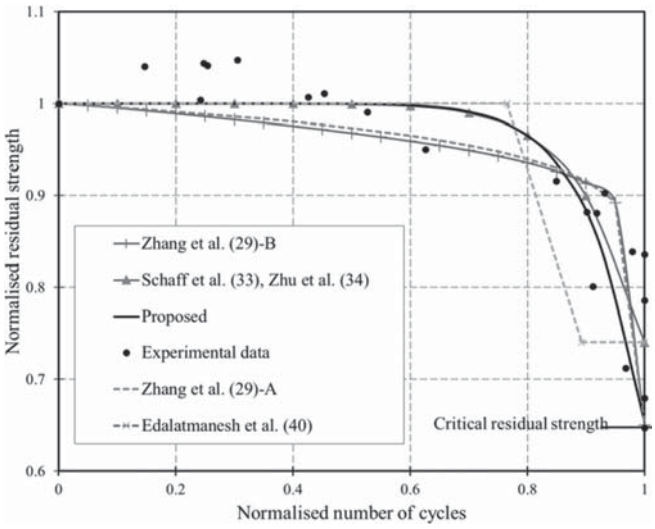

Fig. 12—Normalized concrete strength degradation model.

Using the loading conditions for the experiments conducted and the modified damage model (Eq. (16)), the damage profiles for normalized residual strength and fatigue modulus alongside other residual concrete strength models in the literature[29,33,34,40] were plotted. The residual strength models are shown in Fig. 12. The proposed damage evolution model plot matches well with the Schaff et al.[33] residual strength damage plot. However, toward failure, there is a slightly obvious deviation. This is due to the fact that it is assumed in Schaff et al.[33] that failure will occur at the point where the concrete strength degrades to the maximum fatigue stress applied. On the other hand, the proposed model assumes that failure will occur at a critical damage value based on the experimental observations. Figure 13

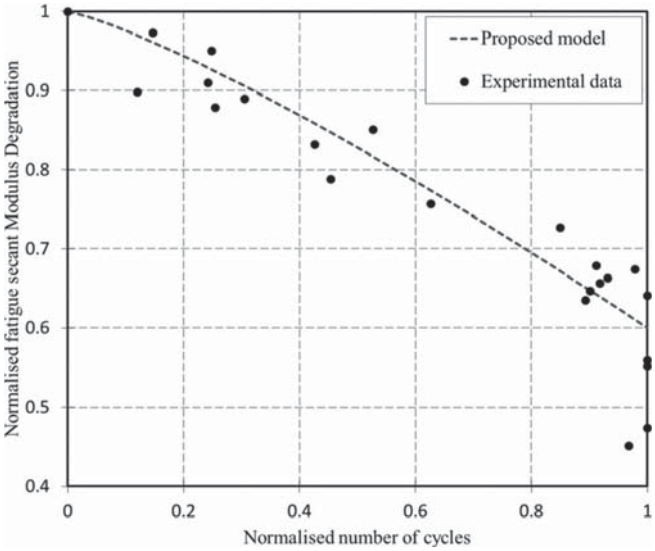

Fig. 13—Normalized fatigue secant modulus degradation model.

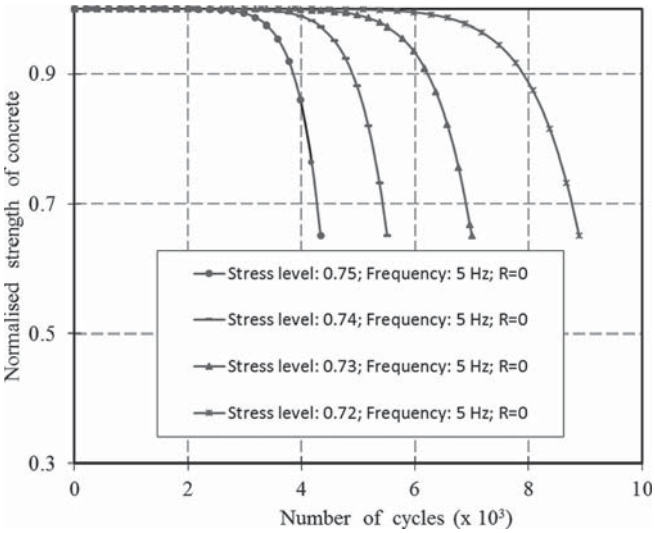

Fig. 14—Effect of stress level on fatigue damage of concrete compressive strength.

also shows the fatigue modulus damage evolution superimposed on the experimental data.

Influence of loading parameters on fatigue damage of concrete

The loading parameters (maximum stress level, frequency, and stress ratio) were varied to observe their effects on the damage evolution of concrete strength using the proposed damage model. The fatigue life that corresponds to the critical damage was estimated using Eq. (9). Figure 14 portrays a delay in damage as the maximum stress level decreases; hence, an increase in the number of cycles to failure. Figures 15 and 16 indicate delays in damage as the frequency and stress ratio increase, respectively. Using the appropriate damage parameter for fatigue modulus (Fig. 11), a similar trend as in the residual strength can also be observed.

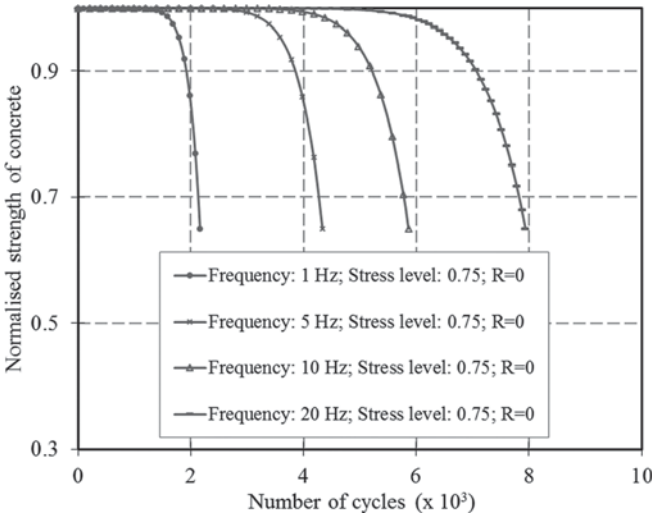

Fig. 15—Effect of frequency on fatigue damage of concrete compressive strength.

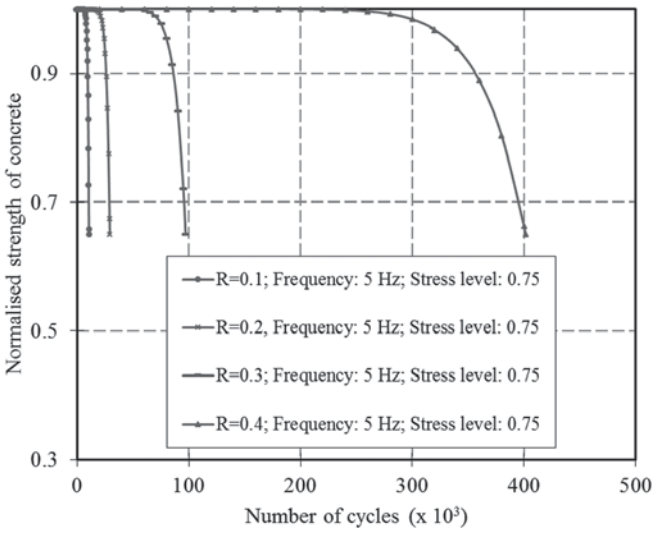

Fig. 16—Effect of stress ratio on fatigue damage of concrete compressive strength.

VARIABLE-AMPLITUDE FATIGUE LOADING

Generally, the fatigue loading of concrete structures are variable in nature. Hence, it is imperative that the proposed damage model accounts for the variability of the fatigue loading in a simple and explicit manner.

The Palngren-Miner Rule[41,42] is commonly used for fatigue damage accumulation when considering variable fatigue loading. The damage per stress level is estimated as the ratio of the number of cycles to the estimated fatigue life. The summation of all estimated damage values gives the total damage. As a criterion for failure, the summation should be equal to 1 or a given critical value.

Basically, the rate of damage accumulation is assumed to be linear; however, a majority of tests conducted and reported in the literature show that fatigue behavior of concrete is nonlinear. In addition, it has been observed that Palmgren-Miner Rule does not account for loading sequence; hence, overly conservative or unconservative predictions have been obtained using the Palmgren-Miner Rule.[3-6]

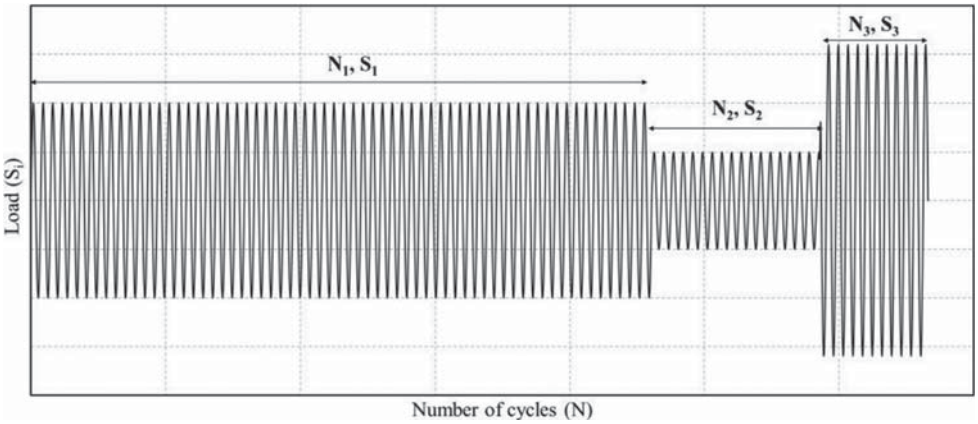

Fig. 17—Stress-cycle diagram for variable amplitude loading.

A procedure similar to that proposed by Schaff and Davidson[33] is described as follows and is illustrated in Fig. 17 and 18. However, experiments on variable fatigue loading of plain concrete specimens are required to verify results obtained from this approach. As an alternative to the estimation of the number of cycles leading to failure using the proposed strain-rate approach or stress life,[38] an approach described by Thun et al.[43] can also be used.

Irrespective of the magnitude of a current stress level S_i, the number of cycles (equivalent number of cycles) that will induce damage equal to a previous damage value can be obtained using the damage model (Eq. (16)). In Fig. 17 and 18, the stresses S_1, S_2, and S_3 are applied for N_1, N_2, and N_3 cycles, respectively. The final damage after the application of S_3 for N_3 cycles can be estimated as follows:

Step 1: Initially, the damage (D_1) due to the first stress level (S_1) and the corresponding number of cycles (N_1) is estimated using the proposed damage model (Eq. (16)).

Step 2: N is calculated by substituting D_1 and the second stress level (S_2) into the damage model (Eq. (16)). The value of N obtained is equal to the equivalent cycles N_{eqv2} for the second load stage. This step converts the previous damage into equivalent cycles.

Step 3: To calculate the damage (D_2) after the second stress level (S_2) fatigue loading, the number of cycles (N_2) for the second stress level is added to N_{eqv2} (equivalent cycles). By substituting the summed cycles ($N_2 + N_{eqv2}$) into the damage model and using the second stress level D_2 for the residual strength is estimated.

Step 4: The third stress level (S_3) is substituted into the damage model to obtain equivalent cycles N_{eqv3}. Subsequently, the value of N in the damage model is replaced by the summation of N_{eqv3} and N_3, as described for D_2 in Step 3.

Step 5: By substituting the summed cycles ($N_3 + N_{eqv3}$) and the third stress level (S_3) in the damage model, D_3 can be estimated.

Based on this concept, the value of the estimated damage takes into account the previous damage. For more variable fatigue loading, this procedure continues until the last variable load is reached. The procedure described for concrete strength under variable fatigue loading can also be used for the residual fatigue secant modulus; hence, similar to residual strength of concrete, the degradation of concrete

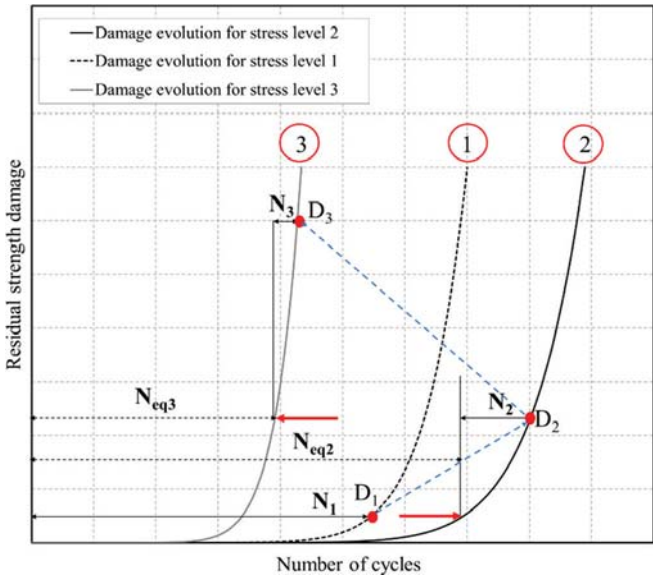

Fig. 18—Damage evolution for variable loading.

fatigue secant modulus can also be predicted appropriately under different loading conditions.

CONCLUSIONS

Based on the results of the experimental and analytical work conducted, the following conclusions were derived:

1. The behavior of concrete elements under fatigue loading can vary greatly and depends on various factors that should be incorporated in the fatigue analysis of concrete for meaningful predictions and results.

2. In the development of the damage models, the use of secondary strain rates of specimens to estimate failure cycles is a reasonable alternative to the use of S-N models.

3. The residual strength and fatigue secant modulus of concrete do not deteriorate to zero as expected in theory; hence, the use of critical damage values is appropriate as observed from experimental results.

4. The evolution of the maximum strain is phased into three stages (normalized profiles in Fig. 3). The three stages are observed from all tested specimens, although the gradients of the evolutions are influenced by the loading parameters (for example, stress level, frequency).

5. The proposed damage models for concrete residual strength and fatigue modulus give reasonable correlations to the observed experimental data and represent an improvement on previously available models, as shown in Fig. 12.

6. Although an approach that accounts for the sequence effect of loading has been proposed for variable fatigue loading, the predictability of this approach requires verification using variable fatigue loading tests of concrete.

7. Further experiments and verifications, especially for very high number of cycles to failure, are required to more fully ascertain the validity of the proposed models.

AUTHOR BIOS

Benard Isojeh *is a PhD Candidate of civil engineering at the University of Toronto, Toronto, ON, Canada. His research interests include the improvement in the design and analysis of wind turbine foundations with a focus on fatigue analysis.*

Maria El-Zeghayar *is a Civil Engineer in the Renewable Power Business Unit at Hatch Ltd, with a specialty in the area of fatigue analysis of materials. She received her PhD from the University of Waterloo, Waterloo, ON, Canada, in 2011.*

Frank J. Vecchio, *FACI, is a Professor at the University of Toronto. He is a member of Joint ACI-ASCE Committees 441, Reinforced Concrete Columns, and 447, Finite Element Analysis of Reinforced Concrete Structures. He received the 1998 ACI Structural Research Award, the 1999 ACI Structural Engineer Award, and the 2011 ACI Wason Medal. His research interests include improved analysis and design of reinforced concrete structures, development of nonlinear analysis procedures, development of constitutive models, and assessment and forensic analysis of concrete structures.*

ACKNOWLEDGMENTS

The authors gratefully acknowledge the Natural Science and Engineering Research Council (NSERC) of Canada and Hatch Ltd for the invaluable contributions and financial support to this research. The authors also acknowledge the assistance received from the Niger Delta Development Commission and the Delta State Government of Nigeria for the duration of this research.

NOTATION

a	=	material parameter
b	=	material parameter
C_f	=	frequency factor
c	=	material constant
D	=	damage
D_{cr}	=	critical damage
E	=	fatigue secant modulus
E_{sec}	=	static secant modulus
f	=	frequency
f_c'	=	compressive strength
K	=	constants (not required in damage model formulation)
k_1	=	constants (not required in damage model formulation)
N	=	number of load cycles
N_{eqv}	=	equivalent cycles
N_f	=	numbers of cycles at failure
S_{max}	=	maximum stress level
s	=	constant parameter
R	=	stress ratio
T	=	period of fatigue cycle
u	=	damage parameter
v	=	damage parameter
β	=	material constant
β_2	=	material constants
γ_2	=	material constants
$\Delta\varepsilon$	=	fatigue strain range
Δf	=	maximum stress level
ε_{cv}	=	strain corresponding to stress range (σ_{max}, σ_{max}) using monotonic stress-strain curve
ε_{sec}	=	secondary strain rate
ζ	=	dimensionless coefficient
σ_{max}	=	maximum stress level
σ_{min}	=	minimum stress level

REFERENCES

1. Shah, S. P., "Predictions of Cumulative Damage for Concrete and Reinforced Concrete," *Materiales de Construcción*, V. 17, No. 1, 1984, pp. 65-68. doi: 10.1007/BF02474059

2. Torrenti, J. M.; Pijaudier-Cabot, G.; and Reynouard, J.-M., eds., *Mechanical Behaviour of Concrete*, John Wiley & Sons, Inc., 2010, pp. 185-223.

3. Papa, E., and Taliercio, A., "Anisotropic Damage Model for the Multiaxial Static and Fatigue Behaviour of Plain Concrete," *Engineering Fracture Mechanics*, V. 55, No. 2, 1996, pp. 163-179. doi: 10.1016/0013-7944(96)00004-5

4. Vega, I. M.; Bhatti, M. A.; and Nixon, W. A., "A Nonlinear Fatigue Damage Model for Concrete in Tension," *International Journal of Damage Mechanics*, V. 4, No. 4, 1995, pp. 362-379. doi: 10.1177/105678959500400404

5. Taliercio, A. L. F., and Gobbi, E., "Experimental Investigation on the Triaxial Fatigue Behaviour of Plain Concrete," *Magazine of Concrete Research*, V. 48, No. 176, 1996, pp. 157-172. doi: 10.1680/macr.1996.48.176.157

6. Song, Y.-P.; Cao, W.; and Meng, X., "Fatigue Properties of Plain Concrete under Triaxial Constant-Amplitude Tension-Compression Cyclic Loading," *Journal of Shanghai University*, V. 9, No. 2, 2005, pp. 127-133. doi: 10.1007/s11741-005-0064-4

7. Tamulenas, V.; Gelazius, V.; and Ramanauskas, R., "Calculation Technique for Stress-Strain Analysis of RC Elements Subjected to High-Cyclic Compression," *Civil and Transport Engineering, Aviation Technologies*, V. 6, No. 5, 2014, pp. 468-473. doi: 10.3846/mla.2014.687

8. Aas-Jacobsen, K., "Fatigue of Concrete Beams and Columns," *Bulletin No. 70-1*, Institutt for Betonkonstruksjoner, Trondheim, Norway, 1970, 148 pp.

9. Murdock, J. W., and Kesler, C. E., "Effects of Range of Stress on Fatigue Strength of Plain Concrete Beams," *ACI Journal Proceedings*, V. 55, No. 2, 1955, pp. 221-231.

10. Hilsdorf, H. K., and Kesler, C. E., "Fatigue Strength of Concrete under Varying Flexural Stresses," *ACI Journal Proceedings*, V. 63, No. 10, Oct. 1966, pp. 1059-1076.

11. Awad, M. E., and Hilsdorf, H. K., "Strength and Deformation Characteristics of Plain Concrete Subjected to High Repeated and Sustained Loads," Civil Engineering Studies, Structural Research Series No. 372, University of Illinois, Champaign, IL, 1971.

12. Oh, B. H., "Cumulative Damage Theory of Concrete under Variable-Amplitude Fatigue Loadings," *ACI Materials Journal*, V. 88, No. 2, Mar.-Apr. 1991, pp. 122-128.

13. Ople, F. S., and Hulsbos, C. L., "Probable Fatigue Life of Plain Concrete with Stress Gradient," *ACI Journal Proceedings*, V. 63, No. 1, Jan. 1966, pp. 59-82.

14. Graf, O., and Brenner, E., "Experiments for Investigating the Resistance of Concrete under often Repeated Compressive Loads 2," *Bulletin* No. 83, Deutscher Ausschuss fur Eisenbeton, 1936.

15. Sparks, P. R., and Menzies, J. B., "The Effect of Rate of Loading upon the Static and Fatigue Strength of Plain Concrete in Compression," *Magazine of Concrete Research*, V. 25, No. 83, 1973, pp. 73-80. doi: 10.1680/macr.1973.25.83.73

16. Raithby, K. D., and Galloway, J. W., "Effect of Moisture Condition, Age, and Rate of Loading on Fatigue of Plain Concrete," *Fatigue of Concrete*, SP-41, American Concrete Institute, Farmington Hills, MI, 1974, pp. 15-34.

17. Holmen, J. O., "Fatigue of Concrete by Constant and Variable Amplitude Loading," *Fatigue of Concrete Structures*, SP-75, American Concrete Institute, Farmington Hills, MI, 1982, pp. 71-110.

18. Naik, T. R.; Singh, S. S.; and Ye, C., "Fatigue Behaviour of Plain Concrete Made with or without Fly Ash," Centre for By-Products Utilization, Department of Civil Engineering & Mechanics, University of Wisconsin-Milwaukee, Milwaukee, WI, 1993.

19. Zhang, B.; Phillips, D. V.; and Wu, K., "Effects of Loading Frequency and Stress Reversal on Fatigue Life of Plain Concrete," *Magazine of Concrete Research*, V. 48, No. 177, 1996, pp. 361-375. doi: 10.1680/macr.1996.48.177.361

20. Takhar, S. S.; Jordaan, I. J.; and Gamble, B. R., "Fatigue of Concrete under Lateral Confining Pressure," *Fatigue of Concrete*, SP-41, American Concrete Institute, Farmington Hills, MI, 1974, pp. 59-70.

21. RILEM COMMITTEE 36-RDL, "Long Term Random Dynamic Loading of Concrete Structures," *Materials and Structures*, V. 17, 1984, pp. 1-28.

22. Hsu, T. C., "Fatigue and Micro-Cracking of Concrete," *Materiales de Construcción*, V. 17, No. 1, 1984, pp. 51-54. doi: 10.1007/BF02474056

23. Hooi, T., "Effects of Passive Confinement on Fatigue Properties of Concrete," *Magazine of Concrete Research*, V. 52, No. 1, 2000, pp. 7-15. doi: 10.1680/macr.2000.52.1.7

24. Lee, M. K., and Barr, B. I. G., "An Overview of the Fatigue Behaviour of Plain and Fibre Reinforced Concrete," *Cement and Concrete Composites*, V. 26, No. 4, 2004, pp. 299-305. doi: 10.1016/S0958-9465(02)00139-7

25. Gebreyouhannes, E.; Kishi, T.; and Maekawa, K., "Shear Fatigue Response of Cracked Concrete Interface," *Journal of Advanced Concrete Technology*, V. 6, No. 2, 2008, pp. 365-376. doi: 10.3151/jact.6.365

26. Cook, D. J., and Chindaprasirt, P., "Influence of Loading History upon the Compressive Properties of Concrete," *Magazine of Concrete Research*, V. 32, No. 111, 1980, pp. 89-100. doi: 10.1680/macr.1980.32.111.89

27. Cook, D. J., and Chindaprasirt, P., "Influence of Loading History upon the Tensile Properties of Concrete," *Magazine of Concrete Research*, V. 33, No. 116, 1981, pp. 154-160. doi: 10.1680/macr.1981.33.116.154

28. Cornelissen, H. A. W., and Reinhardt, H. W., "Effect of Static and Fatigue Preloading on Residual Strength and Stiffness of Plain Concrete," *Fracture Control of Engineering Structures (ECF 6)*, 1987.

29. Zhang, B., and Wu, K., "Residual Fatigue Strength and Stiffness of Ordinary Concrete under Bending," *Cement and Concrete Research*, V. 27, No. 1, 1997, pp. 115-126. doi: 10.1016/S0008-8846(96)00183-4

30. CEB, "Fatigue of Concrete Structures—State of-the-Art-Report," *Bulletin No. 188*, International Federation for Structural Concrete (*fib*), Lausanne, Switzerland, 1988, 312 pp.

31. fib Model Code, 2010, "*fib* Model Code for Concrete Structures," John Wiley & Sons, 2013, 434 pp.

32. Lohaus, L.; Oneschkow, N.; and Wefer, M., "Design Model for the Fatigue Behaviour of Normal-Strength, High-Strength and Ultra-High-Strength Concrete," *Structural Concrete*, V. 13, No. 3, 2012, pp. 182-192. doi: 10.1002/suco.201100054

33. Schaff, J. R., and Davidson, B. D., "Life Prediction Methodology for Composite Structures. Part 1- Constant Amplitude and Two-Stress Level Fatigue," *Journal of Composite Materials*, V. 31, No. 2, 1997, pp. 128-157. doi: 10.1177/002199839703100202

34. Zhu, H., and Li, X., "Experimental Research on Residual Strength of Recycled Aggregate Concrete under Compressive Fatigue Loading," *Advanced Materials Research*, V. 150-151, 2010, pp. 1379-1382. doi: 10.4028/www.scientific.net/AMR.150-151.1379

35. Van Paepegem, W., and Degrieck, J., "A New Coupled Approach of Residual Stiffness and Strength for Fatigue of Fibre-Reinforced Composites," *International Journal of Fatigue*, V. 24, No. 7, 2002, pp. 747-762. doi: 10.1016/S0142-1123(01)00194-3

36. Shah, S. P., and Chandra, S., "Fracture of Concrete Subjected to Cyclic and Sustained Loading," *ACI Journal Proceedings*, V. 67, No. 10, Oct. 1970, pp. 816-827.

37. Gao, L., and Hsu, T. T. C., "Fatigue of Concrete Under Uniaxial Compression Cyclic Loading," *ACI Materials Journal*, V. 95, No. 5, Sept.-Oct. 1998, pp. 575-580.

38. Zhang, B.; Phillips, D. V.; and Green, D. R., "Sustained Loading Effect on the Fatigue Life of Plain Concrete," *Magazine of Concrete Research*, V. 50, No. 3, 1998, pp. 263-278. doi: 10.1680/macr.1998.50.3.263

39. Oneschkow, N., "Influence of Loading Frequency on the Fatigue Behaviour of High-Strength Concrete," Proceedings of the 9th *fib* International PhD Symposium in Civil Engineering, Karlsruhe, Germany, 2012.

40. Edalatmanesh, R., and Newhook, J. P., "Residual Strength of Precast Steel-Free Panels," *ACI Structural Journal*, V. 110, No. 5, Sept.-Oct. 2013, pp. 715-722.

41. Miner, M. A., "Cumulative Damage in Fatigue," *Journal of Applied Mechanics*, V. 12, No. 3, 1945, pp. A159-A164.

42. Palmgren, A., "Die Lebensdauer von Kugellagern," *Zeitschrift des Vereines Deutcher Ingenieure*, V. 68, 1924, pp. 339-341. (VDI Zeitschrift)

43. Thun, H.; Ohlsson, U.; and Elfgren, L., "A Deformation Criterion for Fatigue of Concrete in Tension," *Structural Concrete*, V. 12, No. 3, 2011, pp. 187-197. doi: 10.1002/suco.201100013